JOURNAL OF CATALYSIS 150, 311–320 (1994)

Effect of Prehydrolysis on the Textural and Catalytic Properties of Titania–Silica Aerogels

James B. Miller, Scott T. Johnston,[1] and Edmond I. Ko[2]

Department of Chemical Engineering, Carnegie Mellon University, Pittsburgh, Pennsylvania 15213

Received June 2, 1994; revised August 16, 1994

When applied to the preparation of mixed oxides, sol–gel chemistry affords considerable control over the extent of component mixing: well-mixed oxides result from a preparation in which precursor reactivities are evenly matched. In this work, we describe the preparation and characterization of two sets of mixed titania–silica aerogels covering the entire composition range, one set prepared using prehydrolysis of the silicon precursor to promote homogeneous component mixing and a second set prepared without prehydrolysis. Compared to the prehydrolyzed mixed aerogels, samples prepared without prehydrolysis of the silicon precursor exhibit low 1-butene isomerization activities, low acid site densities, and low fractional Brønsted site populations. These results suggest that the silica and titania components are segregated in the nonprehydrolyzed samples, with inactive silica-rich clusters obscuring much of the surface of a titania-enriched "core." The dependence of important catalytic properties upon composition and homogeneity are explained in terms of the relative number and location of M–O–M′ (cation–oxygen–cation) linkages that exist in a given sample. © 1994 Academic Press, Inc.

INTRODUCTION

Multi-component Oxides and the Role of Homogenety

Many important catalytic properties of metal oxides can be enhanced by introduction of a second oxide component. A minor component can stabilize the major oxide against deterioration of textural properties, most notably surface area and pore volume, upon thermal treatment (1–5). The catalytic activities of mixed oxides have also been reported to be superior to those of the individual components. An important example is the high surface acidity that often develops when dissimilar oxides are combined (1, 2, 4, 6–9).

Both the relative amount of each component oxide and how well the components are mixed affect the textural properties and catalytic performance of the mixed oxide (2, 5, 10–15). But, because traditional preparation techniques do not allow much control of mixing in multicomponent oxides (16), studies that aim to measure directly homogeneity's effects are few. In our laboratory, we prepare mixed-oxide aerogels using the sol–gel method which provides considerable flexibility in controlling component mixing in our samples.

Within the sol–gel process, homogeneity is linked to relative precursor reactivity—well-mixed oxides are associated with evenly matched precursor reactivities. Sol–gel chemistry affords several strategies for adjusting relative precursor reactivity, but by far the most common is prehydrolysis of the less reactive precursor—in essence giving it a "head start" in the hydrolysis–condensation sequence that forms the mixed-oxide network (17). We recently demonstrated, using a set of 95 mol% zirconia-5 mol% silica aerogels, that precursor reactivity matching by prehydrolysis of the silicon precursor, use of a more reactive silicon precursor, and chemical modification of the zirconium precursor all improve mixing thereby causing important changes in the textural, structural, and catalytic properties of the product mixed oxides (5). Specifically, we showed that well-mixed samples were more active as catalysts for isomerization of 1-butene, but generally less effective for stabilizing zirconia against surface area loss and crystallization upon heating.

Titania–Silica Mixed Oxides

Titania has generated significant interest as an SMSI (strong metal–support interaction) support for metals and as a support for vanadia in SCR (selective catalytic reduction) of nitrogen oxides. Titania–silica mixed oxides also display unique properties in these applications (13, 18). Several studies have shown that coprecipitated titania–silicas are more active as catalysts for reactions such as butene isomerization, cumene dealkylation, and 2-propanol dehydration, than either titania or silica alone (18–23). Activity in these reactions has been linked to the mixed oxides' Brønsted acidity (10, 18, 23). Generally, however, titania–silicas have been reported to possess both Lewis and Brønsted acid sites (10, 19, 21, 23, 24).

There have been comparatively few reports of the ef-

[1] Present address: Department of Chemical Engineering, Massachusetts Institute of Technology, Cambridge, MA 02139.

[2] To whom correspondence should be addressed.

0021-9517/94 $6.00

fects of homogeneity on titania–silica catalytic materials. In particular, we are not aware of any work that has addressed the issue of homogeneity over the entire titania–silica composition range. Baiker and co-workers have studied 80 mol% silica-20 mol% titania xerogels (sol–gel-derived materials dried by evaporation) using silica precursor prehydrolysis to promote homogeneous component mixing (25, 26). They observed that well-mixed samples were exclusively *microporous* (14) and were less suitable as supports for vanadia in SCR catalysis than their heterogeneously mixed counterparts (13). Tanabe and co-workers prepared a pair of 90 mol% titania-10 mol% silica samples using variants of the coprecipitation technique—one which promoted homogeneity and one which did not (11). Their homogeneous sample had weaker, *but a higher number*, of acid sites than the heterogeneous sample. In addition, this sample was more active in 1-butene isomerization.

In this work, we describe our preparation and characterization of mixed titania–silica aerogels. By comparing samples prepared with and without prehydrolysis of the silicon precursor, we demonstrate the use of precursor reactivity matching to control homogeneity in mixed samples *over the entire composition range*. We exploit this capability to document the effects of composition and homogeneity in the titania–silica system.

METHODS

Preparation of the Mixed Oxides

Table 1 lists the sol–gel parameters used to prepare the gels described in this work. We have previously documented our preparation of pure titania (27) and silica (28) aerogels.

For a typical prehydrolyzed (PH) mixed-oxide synthesis, tetraethylorthosilicate (TEOS-Aldrich) was first mixed with 40 ml of methanol (Fisher certified) in a 100 ml beaker. Then the nitric acid (Fisher, 70 wt%) and water required for prehydrolysis were added. After stirring with a magnetic bar for a 10 min prehydrolysis period, the titanium precursor, titanium *n*-butoxide (Johnson Matthey), was added. Finally, a second solution containing the water and nitric acid required to complete hydrolysis in 10 ml of methanol was poured into the precursor solution. We define gel-time as the elapsed time between addition of the final solution and the point at which the stirrer can no longer produce a vortex in the reaction mixture.

In a nonprehydrolyzed (NPH) synthesis, the water and nitric acid associated with the silicon precursor were mixed with 40 ml of methanol. Next, the TEOS and titanium *n*-butoxide were added. Immediately thereafter a second solution containing the water and nitric acid associated with the titanium precursor in 10 ml of methanol was poured into the mixed precursor solution. As shown in Table 1, prehydrolysis caused no systematic differences in gel-time.

Each gel was covered with plastic film and allowed to age at room temperature. The 5 mol% silica samples were aged for only 2 hr. The others were aged for 5 days to obtain the structural rigidity required for solvent removal. Removal of the alcohol solvent was accomplished by contact with flowing supercritical (343 K, $\sim 2.2 \times 10^4$ kPa) carbon dioxide in a supercritical extraction screen-

TABLE 1

Sol–Gel Parameters Used in Preparing the Titania–Silica Aerogels

Sample ID[a]	Composition (wt%/mol% silica)	Method (PH or NPH)[b]	$[M^+]$ (mmol/ml MeOH)	$H_2O:M^+$ (mol/mol)[f]	$HNO_3:Ti^{4+}$ (mol/mol)	$HNO_3:Si^{4+}$ (mol/mol)	Gel time (hr : min : sec)
A-TiO_2#101[c]	0/0	N/A[e]	0.625	4.0	0.125	N/A	0:00:43
A-TS96#6	4/5	PH	0.625	4.0	0.050	0.150	0:01:00
A-TS96#18	4/5	NPH	0.625	4.0	0.050	0.150	0:01:20
A-TS73#7	27/33	PH	1.0	4.0	0.050	0.150	0:17:00
A-TS73#11	27/33	NPH	1.0	4.0	0.050	0.150	0:12:00
A-TS57#5	43/50	PH	1.0	4.0	0.025	0.100	>5 hr
A-TS57#10	43/50	NPH	1.0	4.0	0.025	0.100	>10 hr
A-TS40#25	60/67	PH	1.0	4.0	0.014	0.033	>10 hr
A-TS40#32	60/67	NPH	1.0	4.0	0.014	0.033	>10 hr
A-SiO_2#27[d]	100/100	N/A	1.0	4.0	N/A	0.150	N/A

[a] Notation: A = aerogel, TSXX = XX wt% titania, #YY = batch number.
[b] PH = prehydrolyzed, NPH = nonprehydrolyzed.
[c] See Ref. (27) for synthesis' details.
[d] See Ref. (28) for synthesis' details.
[e] Not applicable.
[f] Overall H_2O: (Si^{4+} + Ti^{4+}) ratio and $H_2O:Si^{4+}$ ratio in prehydrolysis step (where applicable).

ing system (Autoclave Engineers, Model 08U-06-60FS). At a CO_2 flowrate of 1400 ccm (ambient conditions), the solvent was completely removed in approximately 2 hr.

The product aerogel was ground to <100 mesh before heat treatment. The first treatment was vacuum drying at 383 K for 3 hr. Each gel underwent an additional vacuum treatment at 573 K to remove tightly bound residual organics. The vacuum treatments were followed by a series of calcinations in flowing oxygen (400 ccm) performed in a tube furnace. Samples were first calcined for 2 hr at 773 K. Further calcinations at 973, 1173, and 1373 K were performed on samples that had previously been heated to 773 K.

Characterization of the Mixed Oxide Aerogels

Pore size distributions, BET surface areas, and pore volumes were measured by nitrogen adsorption/desorption using an Autosorb-1 system (Quantachrome Corp.). Prior to analysis, samples were outgassed under vacuum for 3 hr at 383 K. Crystalline structure was determined by X-ray diffraction (XRD) experiments performed on a Rigaku D/Max Diffractometer using CuK_α radiation.

All samples were tested for their catalytic activity in 1-butene isomerization. Approximately 200 mg of mixed oxide previously calcined to 773 K was used as catalyst in a fixed-bed, downflow reactor. The sample was first dried in 50 sccm helium (Matheson HP) at 473 K for 1 hr. The temperature of the sample was reduced to 423 K and the feed changed to a mixture of 5 sccm 1-butene (Matheson, research grade) and 95 sccm helium. The products—*cis*- and *trans*-2-butene—were quantified by gas chromatography (Gow-Mac 550P with thermal conductivity detector; Supelco 23% SP1700 on 80/20 Chromosorb column). All samples deactivated at low on-stream times, but achieved a steady-state activity by 95 min. We therefore report activity as the isomerization rate, on a per area basis, observed at 95 min time on stream.

Samples calcined to 773 K were examined by diffuse reflectance infrared Fourier transform (DRIFT) spectroscopy using a Mattson Galaxy 5020 FTIR and a Harrick diffuse-reflectance attachment. Spectra were collected over the 400 to 4000 cm^{-1} range with a resolution of 2 cm^{-1} using a DTGS detector. Two types of analyses were performed. In an *ex situ* experiment, the sample was diluted in KBr (~2 wt% mixed oxide) and the spectrum collected at ambient conditions, with no special pretreatment. *Ex situ* experiments were used to probe the silica skeletal vibration portion of the spectrum (~700 to 1200 cm^{-1}).

For *in situ* DRIFT experiments, samples were diluted in KBr (~5 wt%) and placed inside a Harrick reaction chamber. They were then heated under helium flow (~50 ccm) at 473 K for 1 hr and then cooled to 423 K to simulate pretreatment conditions used for 1-butene reactivity testing. For characterization of the hydroxyl region (above ~3000 cm^{-1}), a spectrum was collected after pretreatment, but before exposure to pyridine. Pyridine exposure was carried out at 423 K by diverting helium flow through a pyridine saturator for 15 min. Finally, a spectrum was collected 30 min after termination of pyridine exposure, with the sample still at 423 K and under helium flow. The relative population of Brønsted and Lewis acid sites was determined from the spectrum of adsorbed pyridine following the method of Basila and Kantner (29). We report the results as "fractional Brønsted population," defined as (Brønsted sites)/(Brønsted sites + Lewis sites).

RESULTS

The dependence of BET surface area upon silica content for both prehydrolyzed (PH) and nonprehydrolyzed (NPH) gels after calcination at 773 K for 2 hr is shown in Fig. 1. We find that, at all mixed-oxide compositions, the PH sample has higher surface area than the corresponding NPH sample. The areas of our NPH set are comparable to values reported for coprecipitated titania–silicas (18–21, 30).

Prehydrolysis' effect upon the pore volume of the mixed oxides is shown in Fig. 2. At all mixed-oxide compositions, the PH preparation technique produces higher pore volumes than does NPH. Pore-size distributions for the PH and NPH samples are compared in Fig. 3. Prehydrolysis has little effect upon the distribution's width or the location of its maximum. The most significant difference between PH and NPH pore-size distributions is in

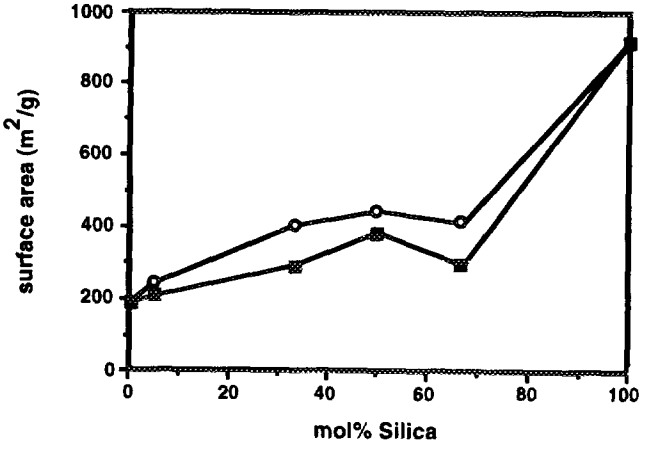

FIG. 1. BET surface area as a function of composition for titania–silica aerogels. Open symbols represent prehydrolyzed samples; closed symbols, nonprehydrolyzed samples. All samples calcined at 773 K in oxygen for 2 hr.

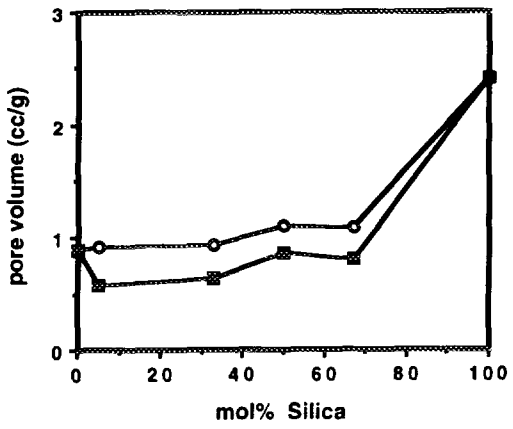

FIG. 2. Pore volume as a function of composition for titania–silica aerogels. Open symbols represent prehydrolyzed samples; closed symbols, nonprehydrolyzed samples. All samples calcined at 773 K in oxygen for 2 hr.

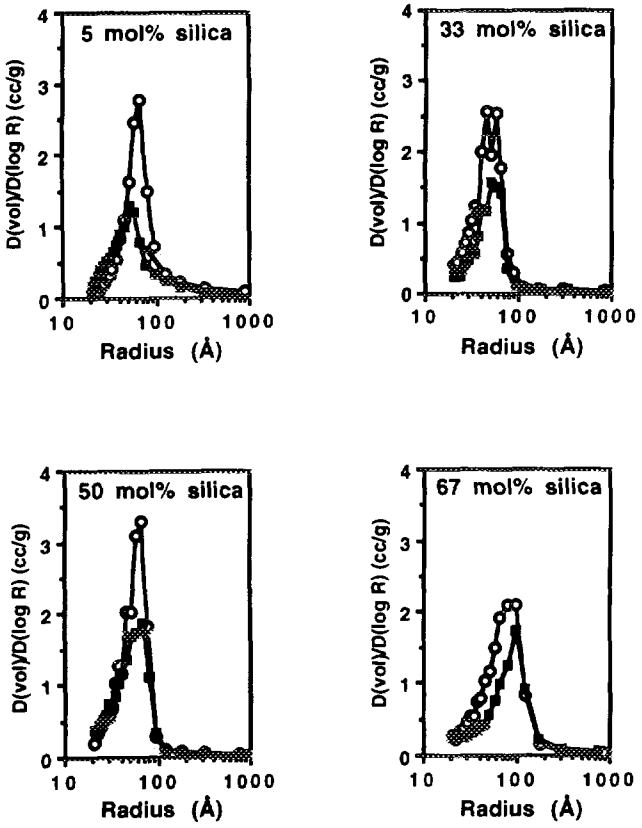

FIG. 3. Pore size distribution as a function of composition for titania–silica aerogels. Open symbols represent prehydrolyzed samples; closed symbols, nonprehydrolyzed samples. All samples calcined at 773 K in oxygen for 2 hr.

total pore volume (the area beneath the distribution curve), as noted above. In contrast to the homogeneous titania-silica xerogels of Baiker *et al.*, which were exclusively microporous (14, 25, 26), all of our samples are mesoporous.

Figure 4 contains the XRD patterns of the PH samples as functions of composition and calcination temperature. For reference, we note that (1) after calcination for 2 hr at only 873 K pure titania aerogel begins to crystallize into the rutile phase (27) and (2) silica aerogel is X-ray amorphous after calcination for 48 hr at 1273 K (28). Figure 4 shows that incorporation of as little as 5 mol% silica into a mixed oxide with titania delays the anatase to rutile transformation to higher temperatures. Furthermore, higher silica contents are even more effective in delaying both the X-ray amorphous to anatase and anatase to rutile transformations. These trends are consistent with literature reports for coprecipitated titania–silicas (1, 3, 18, 19, 20). As Fig. 5 shows, the XRD patterns of the NPH samples are, in general, similar to the corresponding PH patterns. However, note that where titania's anatase and rutile phases coexist—5 mol% silica at 1173 K and 33 mol% silica at 1373 K—rutile peak intensities are greater, relative to the anatase peaks, in the *nonprehydrolyzed* samples.

Figure 6 demonstrates how the 1-butene isomerization activities of the mixed-oxide aerogels vary with composition and preparation technique. All mixed oxides are more active than either of the pure components. And, at all compositions, the PH samples are roughly three times more active, on a per-area basis, than their NPH counterparts. Within both the PH and NPH series, an activity

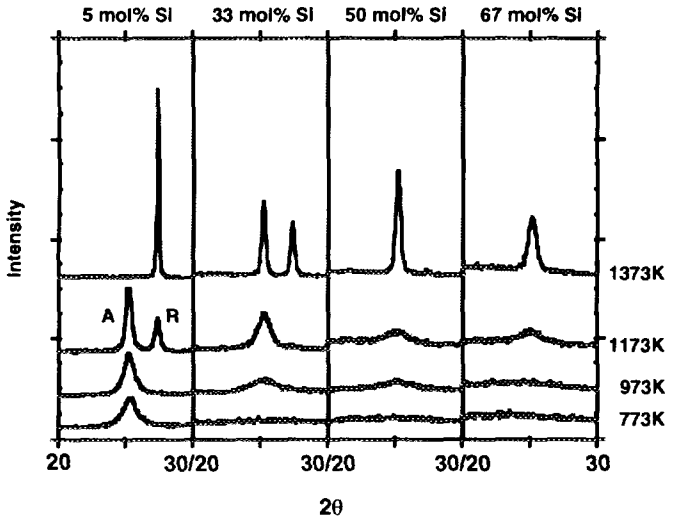

FIG. 4. X-ray diffraction (XRD) patterns for prehydrolyzed titania–silica aerogels. All samples calcined at indicated temperatures in oxygen for 2 hr.

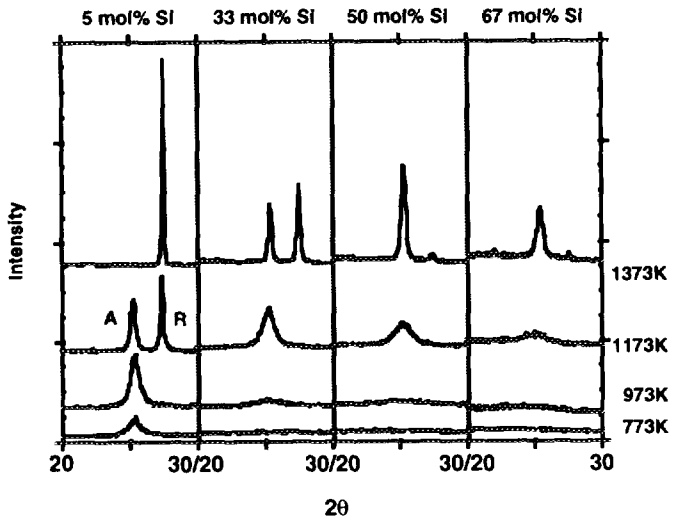

FIG. 5. X-ray diffraction (XRD) patterns for nonprehydrolyzed titania–silica aerogels. All samples calcined at indicated temperatures in oxygen for 2 hr.

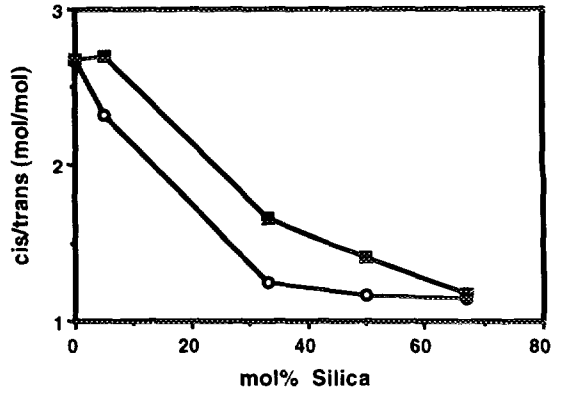

FIG. 7. *cis*-2-Butene/*trans*-2-butene isomerization product ratio as a function of composition for titania–silica aerogels. Open symbols represent prehydrolyzed samples; closed symbols, nonprehydrolyzed samples. All samples originally calcined at 773 K in oxygen for 2 hr. Reaction conditions: 423 K, 1 atm, 5 sccm 1-butene, 95 sccm He, ~200 mg catalyst. Isomer ratios reported at 95 min time on stream.

maximum occurs at 33 mol% silica. Maximum activity for butene isomerization has often been observed at low silica contents (<50 mol%) in titania–silicas (18, 19, 23).

The variations of the *cis*-2-butene/*trans*-2-butene product ratio with mixed-oxide composition for the PH and NPH samples are compared in Fig. 7. At all compositions, NPH samples give slightly higher *cis*/*trans* ratios. And within both series, the ratio decreases with increasing silica content. *Cis*/*trans* ratios in the range of 1 to 2 have been previously reported for 1-butene isomerization over coprecipitated titania–silica catalysts (1, 18), and are indicative of reaction via a butyl carbenium ion intermediate formed at a Brønsted acid site (1, 31, 32). A ratio greater than 2, as observed for our pure titania sample, could be indicative of either (1) a poorly stabilized carbenium ion intermediate (31) or (2) isomerization via a carbanionic intermediate formed at a *basic* site (1, 32).

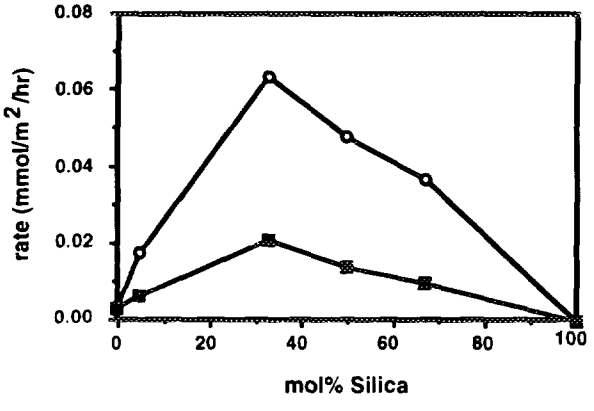

FIG. 6. 1-Butene isomerization activity as a function of composition for titania–silica aerogels. Open symbols represent prehydrolyzed samples; closed symbols, nonprehydrolyzed samples. All samples originally calcined at 773 K in oxygen for 2 hr. Reaction conditions: 423 K, 1 atm, 5 sccm 1-butene, 95 sccm He, ~200 mg catalyst. Isomerization rates reported at 95 min time on stream.

The silica skeletal vibration regions of the *ex situ* DRIFT spectra for selected samples appear in Fig. 8. Our interest is in three features: (1) an asymmetric "Si–O–Si network" vibration at ~1080 cm^{-1} (25, 30, 33–36), (2) the corresponding symmetric motion at ~802 cm^{-1} (25, 30, 37, 38), and (3) a feature at approximately 960 cm^{-1}. In pure silica, the 960 cm^{-1} peak has been assigned to a vibration of silanol (Si–OH) (25, 26). In the mixed oxide, it has been attributed to both silanol (19, 37) and Si–O–Ti bonds in which dilute titanium atoms acquire tetrahedral coordination by isomorphically substituting for silicon in the silica matrix (3, 20, 25, 30, 33, 35–37). While we cannot make a definitive assignment for the 960 cm^{-1} peak in our mixed-oxide samples, we note that our 33 mol% silica samples, which would be expected to have relatively few tetrahedrally coordinated titanium atoms, display substantial 960 cm^{-1} intensity. This observation is consistent with a silanol assignment for the 960 cm^{-1} feature.

Figure 8 shows that the asymmetric Si–O–Si feature moves to lower wavenumber with increasing sample titania content, providing evidence that titania is weakening the silica network (38, 39). The 960 cm^{-1} peak also shifts to lower wavenumber with increasing titania content. Based on a silanol assignment, Sohn and Jang correlated the frequency shift of the 960 cm^{-1} feature with 1-butene isomerization activity (19). They argued that the shift in wavenumber was indicative of a weakening O–H bond which results in enhanced acidity and catalytic activity.

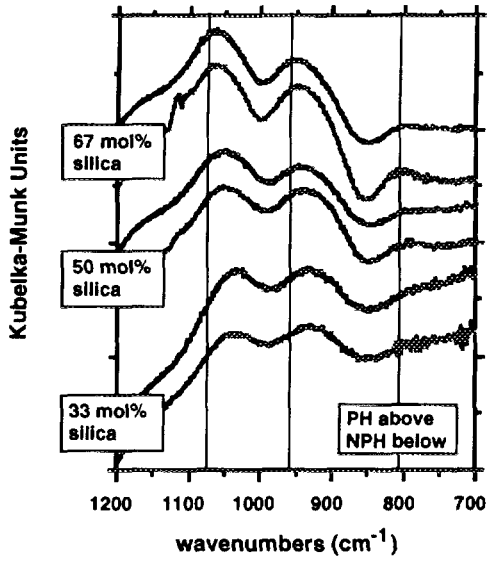

FIG. 8. *Ex situ* skeletal vibration region DRIFT spectra for titania–silica aerogels. All samples calcined at 773 K in oxygen for 2 hr. Reference lines show peak positions for a pure silica aerogel.

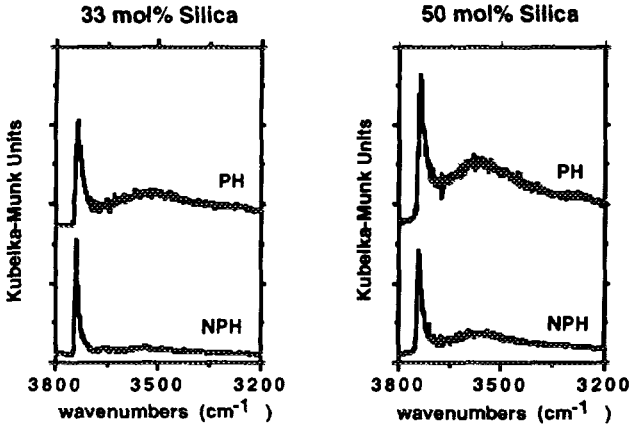

FIG. 10. *In situ* hydroxyl region DRIFT spectra comparing prehydrolyzed and nonprehydrolyzed titania–silica aerogels. All samples originally calcined at 773 K in oxygen for 2 hr.

We note that our spectra are largely unaffected by sample preparation technique. Peak maxima appear at the same wavenumbers for PH and NPH samples of the same composition. However, it is significant that the symmetric Si–O–Si feature (~802 cm^{-1}) in the 67 mol% silica NPH sample—and to a lesser extent in the 50 mol% NPH sample—is more intense than in its PH counterpart. This difference may reflect a degree of separation of the silica and titania components in the NPH sample.

Figure 9 shows the hydroxyl region of the *in situ* DRIFT spectra of the pure-component oxides and the prehydrolyzed mixed oxides. After 773 K calcination and 473 K drying, pure titania aerogel has an insignificant hydroxyl population. In contrast, silica aerogel has a rich hydroxyl region dominated by a high-wavenumber spike that is characteristic of "isolated" -OH groups bound to silicon atoms (23, 40). The spectra of the mixed samples contain two main features. The high wavenumber spike appears in all mixed-oxide samples, even at the lowest silica contents. A second, broader peak appears at lower wavenumbers. As the silica content of the sample increases, this feature grows in intensity and moves to higher wavenumbers. This peak may arise from either (1) hydrogen bonding among densely packed neighboring hydroxyl groups (40) or (2) Ti–OH stretching modes (23, 30, 41).

Figure 10 compares the hydroxyl region of the 33 and

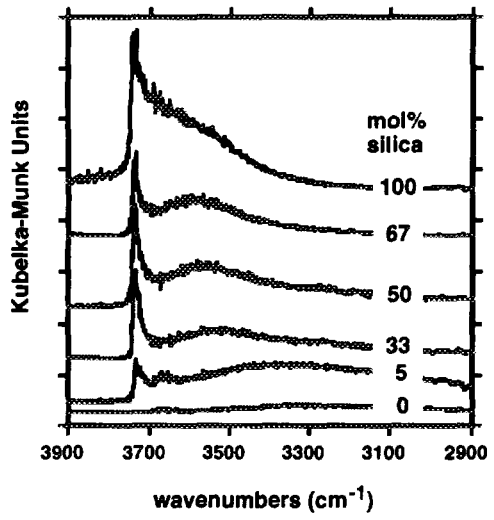

FIG. 9. *In situ* hydroxyl region DRIFT spectra for prehydrolyzed titania–silica aerogels. All samples originally calcined at 773 K in oxygen for 2 hr.

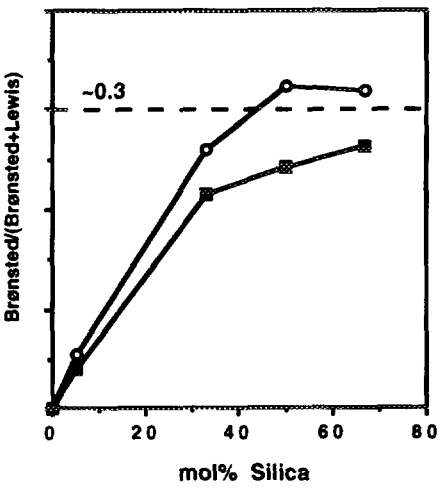

FIG. 11. Fractional Brønsted site population as a function of composition for titania–silica aerogels. Open symbols represent prehydrolyzed samples; closed symbols, nonprehydrolyzed samples. All samples calcined at 773 K in oxygen for 2 hr.

50 mol% silica PH and NPH samples showing that prehydrolysis is associated with a more intense hydrogen-bonded region.

Fractional Brønsted acidity as a function of composition is compared for prehydrolyzed and nonprehydrolyzed samples in Fig. 11. Since it adsorbed no detectable amount of pyridine at *in situ* DRIFT conditions, we conclude that silica aerogel has no acid sites. While all of the mixed oxides have predominantly Lewis sites, we note that prehydrolysis is linked with higher fractional Brønsted populations. In the titania-rich end of the composition range, fraction Brønsted population increases linearly with silica content within both the PH and NPH sample sets. In the middle of the composition range, however, the slopes of both curves decrease markedly, with the prehydrolyzed series exhibiting a maximum fractional Brønsted acidity at 50 mol%.

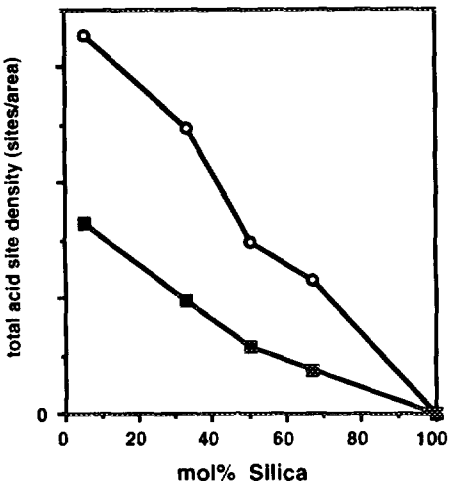

FIG. 12. Calculated total acid site density as a function of composition for titania–silica aerogels. Open symbols represent prehydrolyzed samples; closed symbols, nonprehydrolyzed samples.

DISCUSSION

Effect of Composition on Catalytic Activity and Acidity

As shown in Fig. 6, the mixed oxide that displays the highest activity in 1-butene isomerization—a reaction which probes weak Brønsted sites—contains 33 mol% silica. However, when we consider composition's effect on the relative populations of Brønsted and Lewis acid sites (Fig. 11), we find that less-active samples—those with 50 and 67 mol% silica—have higher fractional Brønsted populations. These observations can be reconciled in terms of changes in total (Lewis + Brønsted) acid site density which occur as a function of composition.

We have estimated relative total acid site densities in our samples in the following manner. First, we assume that isomerization activity is proportional to Brønsted site density. This assumption is reasonable because titania–silica mixed oxides are known to possess strong acid sites (H_0, the Hammett acidity parameter, as low as -8.2) (1), while the isomerization reaction requires only a weak Brønsted acid catalyst ($H_0 < +0.82$) (42). To calculate total relative acid site density, we divide the isomerization activity by the fractional Brønsted content from the DRIFT spectra of adsorbed pyridine (Fig. 11). The results of our estimates appear in Fig. 12. Note that (1) silica aerogel—which adsorbed no pyridine—has no acid sites, (2) for both the PH and NPH sample sets total acid site density increases linearly with titania content, and (3) the PH samples contain roughly twice as many sites as their NPH counterparts. Other researchers have reported total site densities (as determined by titration with ammonia or an alkyl amine) for coprecipitated titania–silicas that increase linearly with increasing titania content up to and occasionally (especially when ammonia is the titrant) including 100% titania (6, 10, 20, 23, 24). The high total acid site densities of the PH samples may also be evidence of their relative homogeneity. As we pointed out earlier, Tanabe and co-workers have linked homogeneity to high acid site densities in coprecipitated titania–silicas (11).

The composition dependencies of acid site density, acid site type, isomerization activity, and hydroxyl inventory can be explained in terms of the relative populations of M–O–M′ linkages that exist on the surface of the mixed oxides. The four main linkage types and some of their important characteristics are listed in Fig. 13. Type A, Ti–O–Ti, exists in pure titania and predominates in the titania-rich mixed oxides. It it easily dehydroxylated, presenting a Lewis acid–Lewis base pair. Since titania aerogel has no Brønsted acidity, the basic site at O^- is responsible for its modest isomerization activity. Titania aerogel's high product *cis*-2-butene/*trans*-2-butene ratio (Fig. 7) is also consistent with isomerization at a basic site on the dehydroxylated surface (1, 31, 32). We note that all silica-containing samples are substantially more active than pure titania (Fig. 6). Presuming comparable site densities, this result suggests that the Brønsted acid sites present in the mixed oxides are more effective for catalyzing the isomerization reaction than are basic sites.

In linkage type B, the dominant hetero linkage in titania-rich samples, the titanium atom retains its single component octahedral coordination. As pointed out by Davis and co-workers (23), this hetero linkage possesses the charge imbalance necessary to create an acid site according to the model proposed by Tanabe (8). In our titania–silica aerogels, this linkage is the source of Brønsted acidity and therefore isomerization activity, consistent with our observation of maximum isomerization activity at a titania-rich composition—33 mol% silica. The hy-

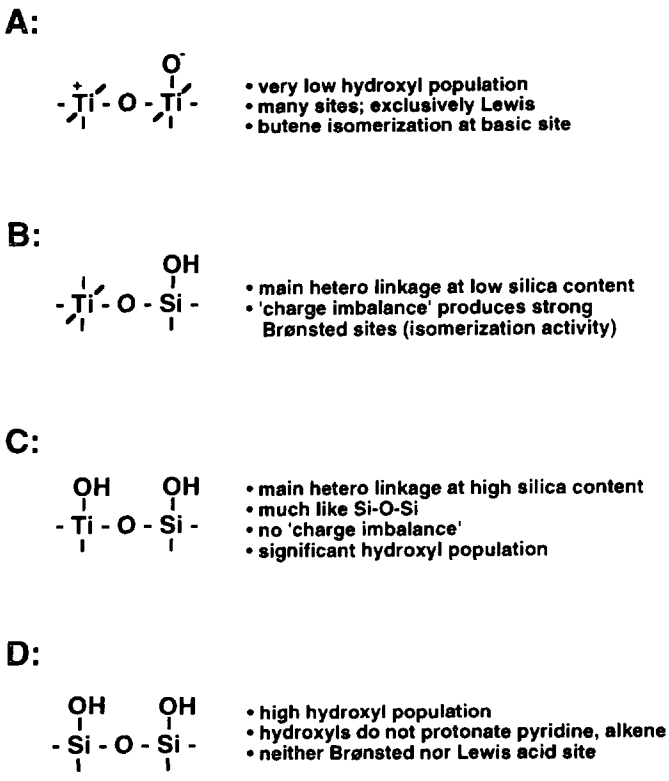

FIG. 13. The four main structural units in titania–silicas and their properties. From top to bottom: (A) the pure titania linkage, (B) hetero linkage with sixfold coordinated titanium atom, (C) hetero linkage with fourfold coordinated titanium atom, and (D) the pure silica linkage.

droxyl region DRIFT spectra (Fig. 9) of the titania-rich mixed oxides are dominated by the high wavenumber "spike," suggesting that this feature is, at least in this composition range, a signature of Brønsted acidity.

Linkage C is the predominant hetero linkage in silica-rich regions. Here, the titanium atom assumes the tetrahedral coordination of the parent silica matrix. Tetrahedrally coordinated titanium has been observed in silica-rich silica–titania glasses and in crystalline titanium silicalite (30, 34, 36, 43). This is the linkage which some groups have tied to the 960 cm^{-1} IR feature. Davis and co-workers (23) pointed out that this structural unit does not possess the charge imbalance required by the Tanabe model for acid site formation (8). Like the Si–O–Si linkage, the hetero linkage with tetrahedrally coordinated titanium probably does not dehydroxylate at the conditions we employ, allowing it to make a significant contribution to the DRIFT hydroxyl region—perhaps as the "broad maximum" that appears at wavenumbers lower than that of the spike.

Type D is the Si–O–Si linkage, found in pure silica and silica-rich mixed oxides. This structural unit does not dehydroxylate at butene isomerization conditions, providing for a very rich hydroxyl region in the DRIFT spectrum. As a potential Brønsted acid, its -OH groups are too weak to protonate either pyridine or 1-butene.

Homogeneity: The Effects of Silicon Precursor Prehydrolysis

Because of their higher *cis–trans* isomerization product ratios (Fig. 7) and lower fractional Brønsted populations (Fig. 11) relative to PH samples of the same composition, we might conclude that NPH sample are, in some manner, surface enriched in *titania*. However, we would also expect titania-rich surfaces to exhibit a higher *total acid site densities*. As Fig. 12 shows, this is clearly not the case; we estimate that NPH samples have roughly half the site densities of their prehydrolyzed counterparts.

We explain these apparently contradictory observations with the following model. Consistent with the core–shell arrangement we would expect of precursors with poorly matched reactivities, *silica* is preferentially located at the surfaces of our NPH samples. As we show in Fig. 14, silica's surface segregation takes the form of "patches" or "clusters" that decorate the surface. These clusters, while not catalytically active themselves (predominantly linkage types C and D), do obscure much of the underlying surface, resulting in low isomerization activities and low total acid sites densities for the NPH sample set. However, in order to create these patches, a material balance requires that silica be borrowed from the subsurface, or core, leaving the subsurface enriched in *titania*. Since it is the unobscured portion of the subsurface which confers acidity and isomerization activity upon the NPH samples, we would predict them to display *cis/trans* ratios and fractional Brønsted populations characteristic of titania enrichment.

The enhanced DRIFT signals for the symmetric silica network vibration (~802 cm^{-1}) displayed by some of our NPH samples (Fig. 8) are also related to component oxide segregation. The silica-rich patches at the NPH sur-

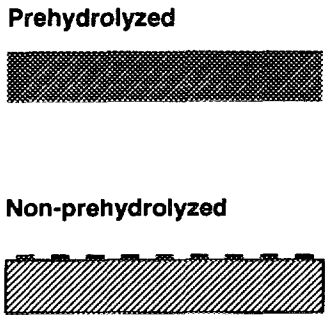

FIG. 14. Models of titania–silica aerogels. Top: in prehydrolyzed samples, silica (black) and titania (white) are homogeneously mixed. Bottom: in nonprehydrolyzed samples, inactive silica clusters obscure large portions of titania-rich core.

face create regions of high Si–O–Si interconnectivity. However, since the actual number of silicon atoms required to form the patches is small, the differences in the DRIFT spectra are subtle.

Likewise, the relative ease with which the NPH samples undergo the anatase to rutile transformation (Figs. 4 and 5) is consistent with our segregation model—we would expect titania-rich regions (the core or subsurface) to accomplish the transition more easily. However, since the type of segregation that we describe affects primarily the surfaces of our samples, its impact upon bulk properties—such as crystalline structure—tends to be much smaller than its influence on surface properties. We note that homogeneity's impact upon crystallization in titania–silica is different from what we have previously reported for 95 mol% zirconia-5 mol% silica aerogels (5). In the zirconia–silica work, we observed that surface-segregated silica was more effective than homogeneously distributed silica for retardation of zirconia's crystallization. The contrast between the behavior of the titania–silica and zirconia–silica systems probably reflects differences in crystallization mechanisms between zirconia and titania. We are currently working with zirconia–silica aerogels having silica contents higher than 5 mol% in order to better understand the differences between the two systems.

Our model (Fig. 14) shares common features with those proposed by Schraml-Marth *et al.* (25). These authors found spectroscopic evidence for domains of titania crystallites in an amorphous silica matrix in titania–silica xerogels prepared without prehydrolysis. Surface segregation of silica also seems to be characteristic of coprecipitated titania–silicas. Several researchers have used X-ray photoelectron spectroscopy (XPS) to measure surface silica concentrations that are significantly in excess of bulk values (20, 30, 43). Earlier, we pointed out the similarity between the surface areas of our NPH sample set and those reported for coprecipitated materials. Collectively, these observations suggest a strong similarity between samples prepared by the two methods. This parallel is not entirely unexpected, since in both techniques a difference in the rates of key processes exists between the titanium and silicon starting materials. For coprecipitation, the rates which differ are the rates of hydroxide precipitation. In the nonprehydrolyzed sol–gel synthesis, the mismatched rates are those of hydrolysis and condensation. By providing prehydrolysis as a simple and effective means to minimize this difference in rates, sol–gel chemistry offers an advantage over coprecipitation for preparation of homogeneous mixed oxides.

While prehydrolysis is the most common precursor reactivity control strategy for sol–gel preparation of mixed oxides, alternatives do exist. Using a set of 95 mol% zirconia-5 mol% silica aerogels, we have recently shown that (1) TEOS prehydrolysis, (2) replacement of TEOS with the more reactive tetramethylorthosilicate (TMOS), and (3) chemical modification of the zirconium precursor with acetylacetone are all effective approaches for minimizing precursor reactivity differences and promoting homogeneous component mixing (5). Based on these results, we expect that both replacement of TEOS with TMOS and modification of the titanium precursor would also be effective for altering homogeneity in titania–silica mixed oxides.

CONCLUSIONS

Within the sol–gel preparation, precursor reactivity matching by prehydrolysis of the silicon precursor is an effective strategy for promoting homogeneity of mixed titania–silica aerogels throughout the entire composition range. This capability allows preparation of materials of constant composition, but differing extents of mixing.

Compared to well-mixed titania–silica aerogels prepared using prehydrolysis, samples prepared without prehydrolysis of the silicon precursor display (1) low activities for 1-butene isomerization, (2) high *cis/trans* isomerization product ratios, (3) low total acid site densities, and (4) low fractional Brønsted site populations. These observations suggest segregation of silica at the surface of NPH samples in the form of inactive silica-rich patches that obscure much of an underlying titania-enriched core.

The composition dependence of important catalytic properties, including acid site density, acid site type (Lewis vs. Brønsted), and activity for 1-butene isomerization, can be explained in terms of the types of M–O–M′ linkages that exist in a given sample. The hetero linkage found in titania-rich environments in which the titanium atom retains its pure component octahedral coordination is responsible for Brønsted acidity and, therefore, 1-butene isomerization activity in the mixed oxides. In silica-rich samples, titanium assumes the tetrahedral coordination of the silica matrix producing hetero linkages without significant acid character.

ACKNOWLEDGMENT

This work is supported by the Division of Chemical Sciences, Office of Basic Energy Sciences, Office of Energy Research, U.S. Department of Energy (Grant DE-FG02-93ER14345).

REFERENCES

1. Itoh, M., Hattori, H., and Tanabe, K., *J. Catal.* **35,** 225 (1974).
2. Sohn, J. R., and Jang, H. J., *J. Mol. Catal.* **64,** 349 (1991).
3. Karmakar, B., and Ganguli, D., *Ind. J. Technol.* **25,** 282 (1987).
4. Maurer, S. M., and Ko, E. I., *Catal. Lett.* **12,** 231 (1992).
5. Miller, J. B., Rankin, S. E., and Ko, E. I., *J. Catal.*, **148,** 673 (1994).

6. Shibata, K., Kiyoura, T., Kitagawa, J., Sumiyoshi, T., and Tanabe, K., *Bull. Chem. Soc. Jpn.* **46,** 2985 (1973).
7. Kijenski, J., and Baiker, A., *Catal. Today* **5,** 1 (1989).
8. Tanabe, K., Sumiyoshi, T., Shibata, K., Kiyoura, T., and Kitagawa, J., *Bull. Chem. Soc. Jpn.* **47**(5), 1064 (1974).
9. Kung, H. H., *J. Solid State Chem.* **52** 191 (1984).
10. Sohn, J. R., and Jang, H. J., *J. Catal.* **136,** 267 (1992).
11. Tanabe, K., Itoh, M., Morshige, K., and Hattori, H., *in* "Preparation of Catalysts" (B. Delmon, P. A. Jacobs, and G. Poncelet, Eds.), p. 65. Elsevier, Amsterdam, 1976.
12. Tanabe, K., Ishiya, C. Matsuzaki, I., Ichikawa, I., and Hattori, H., *Bull. Chem. Soc. Jpn.* **45,** 47 (1972).
13. Handy, B. E., Baiker, A., Schraml-Marth, M., and Wokaun, A., *J. Catal.* **133,** 1 (1992).
14. Handy, B. E., Maciejewski, M., Baiker, A., and Wokaun, A., *J. Mat. Chem.* **2**(8), 833 (1992).
15. Soled S., and McVicker, G. B., *Catal. Today* **14,** 189 (1992).
16. Courty, P., and Marcilly, C., *in* "Preparation of Catalysts" (B. Delmon, P. A. Jacobs, and G. Poncelet, Eds.), p. 119. Elsevier, Amsterdam, 1976.
17. Brinker, C., and Scherer, G., "Sol–Gel Science: The Physics and Chemistry of Sol-Gel Processing." Academic Press, Boston, 1990.
18. Ko, E. I., Chen, J.-P., and Weissman, J. G., *J. Catal.* **105,** 511 (1987).
19. Sohn, J. R., and Jang, H. J., *J. Catal.* **132,** 563 (1991).
20. Imamura, S., Ishida, S., Tarumoto, H., Saito, Y., and Ito, T., *J. Chem. Soc. Faraday Trans.* **89,** 757 (1993).
21. Nakabayashi, H., *Bull. Chem. Soc. Jpn.* **65**(3), 914 (1992).
22. Hattori, H., Itoh, M., and Tanabe, K., *J. Catal.* **38,** 172 (1975).
23. Liu, Z., Tabora, J., and Davis, R. J., submitted for publication.
24. Ingemar-Odenbrand, C., Brandin, J. G. M., and Busca, G., *J. Catal.* **135,** 505 (1992).
25. Schraml-Marth, M., Walther, K. L., Wokaun, A., Handy, B. E., and Baiker, A., *J. Non-Cryst. Solids* **143,** 93 (1992).
26. Walther, K. L., Wokaun, A., Handy, B. E., and Baiker, A., *J. Non-Cryst. Solids* **134,** 47 (1991).
27. Campbell, L. K., Na, B. K., and Ko, E. I., *Chem. Mater.* **4,** 1329 (1992).
28. Maurer, S. M., Ph.D. Thesis, Carnegie Mellon University, 1991.
29. Basila, M. R. and Kantner, T. R., *J. Phys. Chem.* **70,** 1681 (1966).
30. Ingemar-Odenbrand, C., Andersson, S. L. T., Andersson, L. A. H., Brandin, J. G. M., and Busca, G., *J. Catal.* **125,** 541 (1990).
31. Goldwasser, J., Engelhardt, J., and Hall, W. K., *J. Catal.* **71,** 381 (1981).
32. Kung, H. H., "Transition Metal Oxides: Surface Chemistry and Catalysis." Elsevier, Amsterdam, 1989.
33. Yuan, L., and Yao, G., *J. Non-Cryst. Solids* **100,** 309 (1988).
34. Hayashi, T., Yamada, T., and Saito, H., *J. Mater. Sci.* **18,** 3137 (1983).
35. Cheng, J., and Wang, D., *J. Non-Cryst. Solids* **100,** 288 (1988).
36. Liu, Z., and Davis, R. J., *J. Phys. Chem.* **98,** 1253 (1994).
37. Perry, C., and Li, X., *in* "Eurogel '91" (S. Vilminot, R. Nass, H. Schmidt, Eds.), p. 461. Elsevier, Amsterdam, 1992.
38. West, J., and Cheng, Y. C., *SPIE Sol–Gel Optics I* **1758,** 55 (1992).
39. Best, M., and Condrate, R., *J. Mater. Sci. Lett* **4,** 994 (1985).
40. Little, L. H., "Infrared Spectra of Adsorbed Species." Academic Press, London, 1966.
41. Hair, M. L., "Infrared Spectroscopy in Surface Chemistry." Dekker, New York, 1967.
42. Jacobs, P. *in* "Characterization of Heterogeneous Catalysts" (F. Delanny, Ed.), p. 367. Dekker, New York, 1984.
43. Stakheev, A., Shpiro, E., and Apijok, J., *J. Phys. Chem.* **97,** 5668 (1993).